Development 135, 2139-2149 (2008) doi:10.1242/dev.016725

C3G regulates cortical neuron migration, preplate splitting and radial glial cell attachment

Anne K. Voss[1,2,*], Joanne M. Britto[3], Mathew P. Dixon[1], Bilal N. Sheikh[1,2], Caitlin Collin[1], Seong-Seng Tan[3] and Tim Thomas[1,2,*]

Neuronal migration is integral to the development of the cerebral cortex and higher brain function. Cortical neuron migration defects lead to mental disorders such as lissencephaly and epilepsy. Interaction of neurons with their extracellular environment regulates cortical neuron migration through cell surface receptors. However, it is unclear how the signals from extracellular matrix proteins are transduced intracellularly. We report here that mouse embryos lacking the Ras family guanine nucleotide exchange factor, C3G (Rapgef1, Grf2), exhibit a cortical neuron migration defect resulting in a failure to split the preplate into marginal zone and subplate and a failure to form a cortical plate. C3G-deficient cortical neurons fail to migrate. Instead, they arrest in a multipolar state and accumulate below the preplate. The basement membrane is disrupted and radial glial processes are disorganised and lack attachment in C3G-deficient brains. C3G is activated in response to reelin in cortical neurons, which, in turn, leads to activation of the small GTPase Rap1. In C3G-deficient cells, Rap1 GTP loading in response to reelin stimulation is reduced. In conclusion, the Ras family regulator C3G is essential for two aspects of cortex development, namely radial glial attachment and neuronal migration.

KEY WORDS: Neuronal migration, Cerebral cortex, Radial glia, Reelin, Cell adhesion, Ras signalling pathway, Mouse

INTRODUCTION

The development of the cerebral cortex into a six-layered structure involves a coordinated series of events. Disruption of these events leads to mental retardation syndromes including lissencephaly (Ayala et al., 2007). Neural precursors proliferate in the ventricular and subventricular zones, exit the cell cycle and migrate to specific locations. At the commencement of corticogenesis, cells from the cortical hem and the cortical ventricular zone migrate to the pial surface to form the cortical preplate (Bielle et al., 2005; Takiguchi-Hayashi et al., 2004). The next cohort of cells arises from the cortical ventricular zone and forms layer VI neurons. These cells position themselves in the centre of the preplate, thus splitting the preplate into the marginal zone/layer I and the subplate (Bayer and Altman, 1991; Gupta et al., 2002). These early steps of cortical development are glia-independent and entail the translocation of the nuclei and cell bodies by contracting cell processes anchored at the pial basement membrane (Gupta et al., 2002; Nadarajah et al., 2001; Olson and Walsh, 2002). The succeeding cohorts of cells successively migrate through previously formed layers and position themselves superficially such that layers VI, V, IV and II/III develop in an inside-out fashion (Bayer and Altman, 1991; Gupta et al., 2002). These later steps involve migration of cortical neurons along radial glial cells, which extend cell processes from their ventricular position to the pial surface, where they are anchored in the basement membrane (Gupta et al., 2002; Olson and Walsh, 2002). Clearly, neuronal migration relies on the interaction of neurons with their extracellular environment, including neighbouring cells (radial glia) and the extracellular matrix (ECM) proteins in the basement membrane.

The ECM is a network of proteins that forms a scaffold providing mechanical support, but ECM proteins also are essential inducers of cell signalling. The ECM contains specialised components in defined regions specifically for cell signalling. For example, ECM within the marginal zones of the cerebral cortex and the cerebellum contains reelin, which regulates neuronal migration (D'Arcangelo et al., 1995). Other ECM proteins such as laminin, fibronectin and collagen, are produced by the neuroepithelium throughout neurogenesis (Liesi, 1985; Sheppard et al., 1991; Stewart and Pearlman, 1987; Thomas and Dziadek, 1993b). Here we provide functional evidence that C3G (Rapgef1, Grf2), a molecule that transduces signals from ECM proteins, is essential for cortical neuron migration.

C3G is a guanine nucleotide exchange factor for small GTPases of the Ras family (Knudsen et al., 1994; Tanaka et al., 1994). C3G can be activated by a number of extracellular signals including integrin binding (Arai et al., 2001; Arai et al., 1999; Uemura and Griffin, 1999) and reelin stimulation (Ballif et al., 2004). Phosphorylation of C3G and complex formation with the adaptor protein Crk are necessary for C3G activation (Ichiba et al., 1997). The Crk-C3G complex translocates to the cytoplasmic membrane (Ichiba et al., 1997), where C3G stimulates GTP exchange predominantly on Rap1 (Ohba et al., 2001), thereby activating signalling through Rap1. C3G regulates migration in fibroblasts (Ohba et al., 2001; Voss et al., 2003) and is essential for filopodia formation and cytoskeletal changes in fibroblasts (Radha et al., 2007). In addition, C3G regulates neural precursor proliferation in the developing cerebral cortex (Voss et al., 2006).

We report here that during the development of the cerebral cortex, C3G is essential for normal neuronal migration.

MATERIALS AND METHODS

Animals, BrdU treatment, embryo recovery and tissue processing

Experiments were undertaken with the approval of the Royal Melbourne Hospital Research Foundation Animal Ethics Committee and conforming to the Australian Code of Practice for the Care and Use of Animals for Scientific Purposes. Noon of the day of vaginal plug detection was defined

[1]Walter and Eliza Hall Institute of Medical Research, Parkville, Victoria 3050, Australia. [2]Department of Medical Biology, University of Melbourne, Parkville 3010, Victoria, Australia. [3]Howard Florey Institute, Parkville, 3010 Victoria, Australia.

*Authors for correspondence (e-mails: avoss@wehi.edu.au; tthomas@wehi.edu.au)

Accepted 18 April 2008

as embryonic day 0.5 (E0.5) in timed matings of $C3G^{gt/+} \times C3G^{gt/+}$ mice (Voss et al., 2003) on a CD1 or a CBA background. BrdU experiments were carried out as previously described (Thomas et al., 2000). Embryos were recovered, genotyped and processed for histology as reported previously (Voss et al., 2003).

Antibodies

Primary antibodies were directed against BrdU (Bio-Science Products 010198, 1:10), β-tubulin type III (Promega G7121, 1:2000), calretinin (Chemicon AB5054, 1:100), Emx1 (Chan et al., 2001), laminin (Chemicon AB2034, 1:1000), Map2 (Sigma M4403, 1:200), reelin (Abcam ab18570, 1:1000), RC2 (from Miyuki Yamamoto via the Developmental Studies Hybridoma Bank, 1:200), C3G (Santa Cruz sc-869 and sc-15359, 1:500) and phospho-tyrosine (BD Transduction Laboratories PY-20, 1:1000). Secondary antibodies were Vector Laboratories BA-1400, Vector FI-2020, Molecular Probes A-21124, A-11004, A-11035, A-11029, A-11003, A-11001, Southern Biotechnology 710003 and Jackson ImmunoResearch 111-156-003.

Immunoprecipitation, immunoblotting and affinity purification

Rap1 activation assays were conducted as described previously (Voss et al., 2006). Immunoblotting was performed as described (Voss et al., 2003; Voss et al., 2006). C3G immunoprecipitations were performed as described (Ballif et al., 2004). Briefly, cortical neurons were washed with ice-cold PBS, lysed in 400 μl nRIPA [0.15 M NaCl, 1% Triton X-100, 0.1% SDS, 1% sodium deoxycholate, 10 mM sodium phosphate (pH 7.4), 2 mM EDTA, 14 mM 2-mercaptoethanol, 50 mM NaF, 2 mM Na_3VO_4, 1 mM phenylarsine oxide and one complete protease inhibitor tablet per 40 ml]. Lysates were clarified by centrifugation and then precleared with a cocktail of protein A/protein G sepharose [protein A (G) sepharose 4 fast flow, GE Health Care]. Lysates were mixed with 20 μl protein G sepharose and 2 μg anti-C3G (sc-15359) antibody. Samples were incubated for 2.5 hours with agitation at 4°C. Resin was washed three times with 0.8 ml nRIPA buffer. Samples were eluted by boiling in 30 μl 2× sample buffer [4% SDS, 124 mM Tris-HCl (pH 6.8), 0.1% Bromophenol Blue, 20% glycerol, 200 mM DTT).

In situ hybridisation and immunofluorescence

In situ hybridisation and BrdU detection were performed as described (Thomas et al., 2000). Immunofluorescence on sections was carried out as described (Voss et al., 2003). Immunofluorescence on cultured cells was performed as described (Merson et al., 2006; Voss et al., 2000).

Cell culture and cell transfection

Neural precursor cells were cultured in neural stem cell proliferation medium as previously described (Merson et al., 2006). Human 293T cells were transfected with 4.5 μg of either pCRL [reelin expression vector; gift from T. Curran (D'Arcangelo et al., 1997)] or pCDNA3.1 (empty parental vector; mock) using FuGENE (Roche). Medium was replaced 24 hours post-transfection with neural differentiation medium (as neural stem cell proliferation medium but without Fgf2, and without Egf). Conditioned medium was recovered 48 hours post-transfection. Cortical neurons were isolated and cultured as described (Herrick and Cooper, 2002). Briefly, E16.5 cerebral hemispheres were dissociated enzymatically and mechanically, passed through a sieve, collected by centrifugation and plated onto poly-L-lysine-coated tissue culture plates in neural differentiation medium with 1% foetal bovine serum.

Organotypic brain slice cultures and confocal time-lapse imaging

Replication-incompetent enhanced GFP (eGFP)-expressing retrovirus was produced from a stably transfected packaging cell line, 293gp NIT-GFP (gift from F. Gage, Salk Institute, La Jolla, CA). Cells were transiently transfected with pVSV-G (Palmer et al., 1999), the supernatant harvested after 48 hours and concentrated by ultracentrifugation at 53,000 ***g*** for 3.5 hours at 4°C.

Coronal slices were prepared from embryonic forebrain as previously described (Noctor et al., 2001). Slices were obtained from the anterior half of the cerebral hemispheres, where medial and lateral ganglionic eminences could be separately identified, and cultured individually on slice culture inserts (Millicell, Millipore). Cultured slices were incubated for 48 hours with eGFP-expressing retrovirus before images were collected on an inverted Zeiss Axiovert 200-LSM 5 Pascal confocal microscope using 488 nm excitation and LP 505-530 nm emission filters. Images were captured using a 10× objective set at the sectional plane that contained the majority of migrating cells (optical slice <10 μm). Time-lapse imaging was performed at 37°C, 100% relative humidity, 5% CO_2 in air on a CO_2- and heat-controlled stage incubator (Zeiss) using minimum laser exposure to prevent photo-damage and bleaching. Images were taken every 15 minutes for 6 to 12 hours.

Cortical neuroepithelial explant cultures and time-lapse imaging

Telencephalic hemispheres were isolated and cultured on Matrigel or laminin as described previously (Thomas and Dziadek, 1993a). For time-lapse imaging, telencephalic hemisphere explants on Matrigel were cultured on an inverted imaging microscope (Zeiss) equipped with a heat-controlled stage incubator at 37°C, 100% relative humidity and 5% CO_2 in air. Images were taken every 5 minutes for 22 hours in phase contrast using a 20× objective. The imaging interval of 22 hours was taken from day 3 to day 4 after plating.

Statistical data analysis

Data were analysed using StatView 5.0.1 Software (SAS Institute), performing analyses of variance followed by Fisher's post-hoc tests or χ^2 test as indicated in the tables. The default alpha value of the software (5%) was used. Data are presented as mean ± s.e.m.

RESULTS

The *C3G* gene is expressed in the developing cerebral cortex

During development, *C3G* is expressed at low levels in all cell types (Voss et al., 2003) and at higher levels in the developing nervous system (Voss et al., 2006). In the cortical neuroepithelium, *C3G* expression was observed at low levels in proliferating ventricular zone cells at E12.5 and E15.5 (Fig. 1A-F). Differentiating neurons near the pial surface at E12.5 (Fig. 1A-C) and in the cortical plate at E15.5 (Fig. 1D-F) expressed slightly higher levels of *C3G* mRNA.

C3G$^{gt/gt}$ mutants show morphological defects in the developing cerebral cortex in vivo

Mice homozygous for a *C3G*-null allele do not survive beyond E5.5 (Ohba et al., 2001). We studied the role of C3G later in development, using a hypomorphic mutant *C3G* allele ($C3G^{gt}$) that expresses less than 1% normal *C3G* mRNA and less than 5% normal C3G protein (Voss et al., 2003). C3G is required for blood vessel maturation and, on a 129Sv-enriched background, the level of C3G protein produced by the $C3G^{gt}$ mutant allele is insufficient for the differentiation of blood-vessel-supporting cells, resulting in haemorrhage in the majority of homozygous mice (80%) by E11.5 (Voss et al., 2003). However, we found that crossing the $C3G^{gt}$ allele onto an outbred CD1 background or to a CBA inbred background ameliorated the blood vessel fragility phenotype. On these vigorous genetic backgrounds, all homozygous embryos live beyond E12.5, the majority are externally indistinguishable from wild-type littermate controls at E12.5 and are alive at E14.5. This provided the opportunity to study the requirements for C3G during the early development of the cerebral cortex.

The $C3G^{gt/gt}$ mutant cortical neuroepithelium was histologically indistinguishable from wild-type littermate controls at E9.5, E10.5 and E11.5 (not shown). At E12.5, the $C3G^{gt/gt}$ cortical neuroepithelium lacked a continuous basement membrane, which was visible by differential interference contrast microscopy in wild-type controls (arrows, Fig. 1G, versus arrowheads, Fig. 1H). At E13.5, $C3G^{gt/gt}$ neuroepithelial cells (arrowheads, Fig. 1J) could be seen in the area of the pericerebral vascular complex, a tissue

structure outside of the neuroepithelium, which is demarcated in wild-type controls (stippled line, Fig. 1I). At E14.5, the developing wild-type cortical primordium was clearly organised in a ventricular zone with radially oriented neuroepithelial cells, an intermediate zone and a nascent cortical plate, the primordium of the cerebral cortex (Fig. 1K). The subplate was positioned between the intermediate zone and the cortical plate. The marginal zone overlay the cortical plate on its pial surface (Fig. 1K). By comparison, the *C3G*$^{gt/gt}$ cerebral cortex primordium appeared disorganised (Fig. 1L). The subplate was indistinct and, consequently, the boundary between the intermediate zone and the cortical plate was not distinguishable. A cortical plate or a marginal zone could not be discerned (Fig. 1, compare K with L). *C3G*$^{gt/gt}$ cortical cells lacked radial orientation and appeared rounded (Fig. 1, compare M with N). The defects in cerebral cortex development were consistently observed in a total of 21 *C3G*$^{gt/gt}$ mutant embryos but not in 21 wild-type controls at E12.5 (four pairs), E13.5 (ten pairs) and E14.5 (seven pairs). Our findings suggest that C3G deficiency is incompatible with normal development of the cerebral cortex.

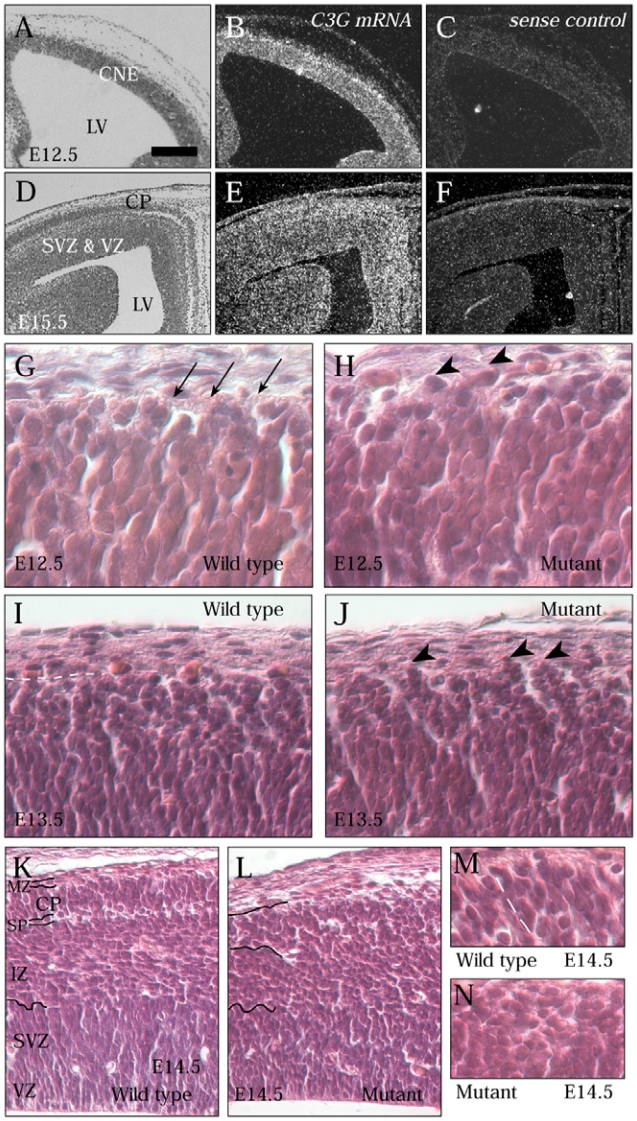

Fig. 1. *C3G* expression and histology of the developing cerebral cortex of the *C3G*$^{gt/gt}$ mutant. (**A-F**) In situ hybridisation using a *C3G*-specific cRNA probe (A,B,D,E) or sense control probe (C,F) on adjacent sections of wild-type mouse cerebral cortex at E12.5 (A-C) and E15.5 (D-F). Bright-field (A,D) and corresponding dark-field (B,E) images. Silver grains representing *C3G* mRNA distribution appear white in the dark-field image (B,E,C,F). (**G-N**) Haematoxylin and Eosin stained paraffin sections of wild-type (G,I,K,M) and *C3G*$^{gt/gt}$ mutant (H,J,L,N) developing cerebral cortex at E12.5 (G,H), E13.5 (I,J) and E14.5 (K-N). Images were taken using differential interference contrast optics, which reveal unstained or weakly stained structures. Arrows in G indicate basement membrane and arrowheads in H the lack thereof. Stippled line in I indicates the demarcation between the neuroepithelium and the pericerebral tissue; arrowheads in J indicate neuroepithelial cells invading the pericerebral space. Dashed line in M indicates ventricular-to-pial orientation of cortical plate cells. CNE, cortical neuroepithelium; CP, cortical plate; IZ, intermediate zone; LV, lateral ventricle; MZ, marginal zone; SP, subplate; SVZ, subventricular zone; VZ, ventricular zone. Scale bar: 197 μm in A-C; 94 μm in D-F; 13 μm in G,H; 32 μm in I,J; 38 μm in K,L; 18 μm in M,N.

The *C3G*$^{gt/gt}$ mutant basement membrane is disrupted and neurons protrude into the pericerebral space

Microtubule-associated protein 2 (Map2; Mtap2 – Mouse Genome Informatics) is a marker of post-mitotic neurons and identifies cortical neurons in the developing cerebral cortex. In the wild type, Map2 staining was stronger in neurons within the cortical plate than in migrating neurons in the intermediate zone, and marked the cortical plate clearly (Fig. 2A). Although strongly Map2-positive cortical neurons were present in the *C3G*$^{gt/gt}$ cortex (Fig. 2B), they were disorganised and not structured into a cortical plate (Fig. 2, compare A with B; n=7 each for wild-type and *C3G*$^{gt/gt}$ brains at E13.5 and E14.5).

We examined the basement membrane integrity by laminin immunofluorescence staining of *C3G*$^{gt/gt}$ mutant and wild-type developing cortex (n=3 for each genotype at each developmental stage totaling nine *C3G*$^{gt/gt}$ mutant and nine wild-type brains). As expected, laminin immunoreactivity was strongest in the area of the basement membrane and was also seen associated with blood vessels. In the wild type, laminin was continuous, encircling the entire neuroepithelium at its pial surface marking the basement membrane (Fig. 2C). In the *C3G*$^{gt/gt}$ mutants, laminin deposition appeared initially irregular (Fig. 2D) and then areas with and without laminin alternated along the pial surface (Fig. 2E). These two stages of disintegration of the basement membrane were seen in *C3G*$^{gt/gt}$ mutants at E12.5 and E13.5. At E14.5, the latter, more severe stage of basement membrane disintegration prevailed. Furthermore, cells were found to protrude from the neuroepithelium into the pericerebral space (arrow, Fig. 2G). Map2 staining (arrow, Fig. 2B) and Map2/laminin double staining (arrows, Fig. 2G,I) showed that the cells protruding into the pericerebral space were of neuronal identity. A possible cause of the heterotopic position of neuronal cells in the pericerebral space is the basement membrane disintegration.

C3G$^{gt/gt}$ mutants exhibit cortical neuron migration defects in vivo resulting in a failure of preplate splitting

At E10.5, the first neurons are born, migrate to the pial surface and form the cortical preplate, which can be seen between E12.5 and E13.5. These preplate cells can be observed in their final destination after incorporation of the thymidine analogue BrdU during the DNA-synthesis phase of their last cell division at E10.5. The next cohort of neurons leave the cell cycle at E11.5, migrate from the ventricular zone towards the pial surface and position themselves in the centre of the preplate, thereby splitting the preplate into marginal

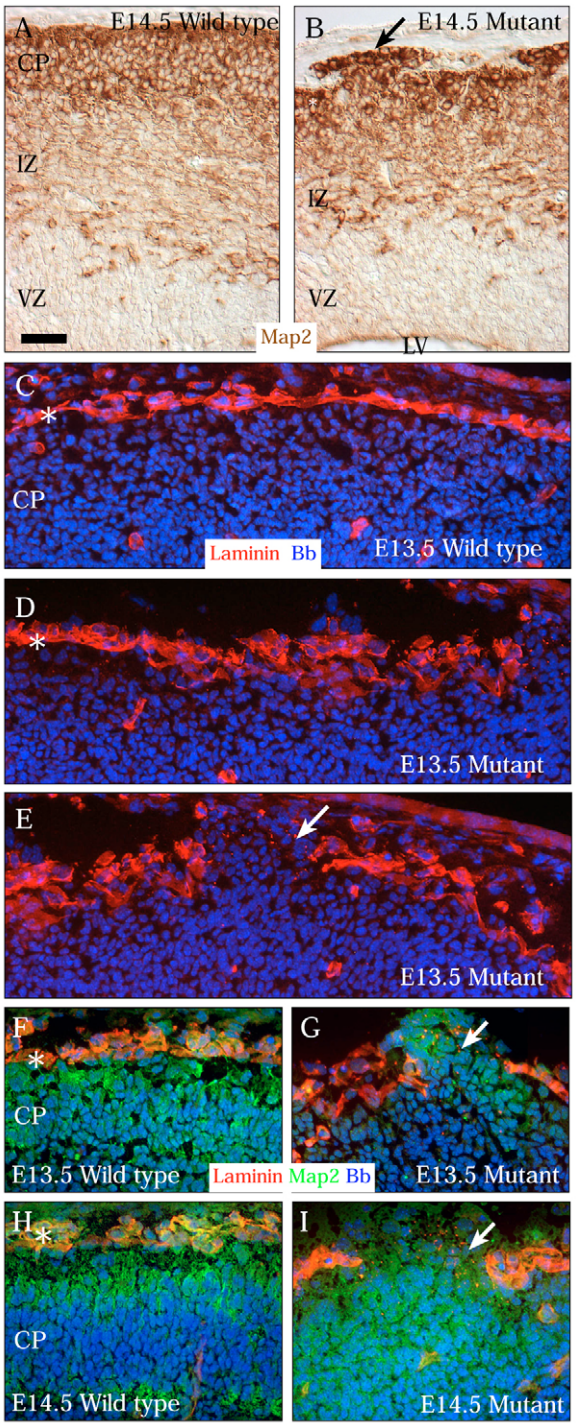

Fig. 2. Abnormal cortical plate development in *C3G*$^{gt/gt}$ mutant mouse embryos. (**A-I**) Wild-type (A,C,F,H) and *C3G*$^{gt/gt}$ mutant (B,D,E,G,I) developing cerebral cortex, at E13.5 and E14.5 as indicated, stained for the neuronal marker Map2 (brown in A,B; green in F-I) and/or laminin (red in C-I) and counterstained with bisbenzimide (blue in C-I). *C3G*$^{gt/gt}$ mutants show disorganisation of the cortical plate and invasion of the pericerebral space by neurons (arrow in B). E13.5 developing cortex shows continuity of laminin staining along the basement membrane (asterisk) in the wild type (C) and the disorganisation (D) and discontinuity (arrows in E) of laminin staining in the E13.5 *C3G*$^{gt/gt}$ mutant, as well as nuclei (blue) of cells protruding into the basement membrane gaps (arrow in E). The cells protruding into the basement membrane gaps are positive for the neuronal marker Map2 (arrows). Labels as in Fig. 1. Scale bar: 29 μm in A,B; 35 μm in C-I.

zone and subplate, which can be seen at E14.5. If the preplate cells have been labelled with BrdU previously, the products of preplate splitting, the marginal zone and the subplate, are visible as two distinct layers containing BrdU-labelled cells. Cells that leave the cell cycle after BrdU label incorporation are strongly BrdU positive. By contrast, cells remaining in the cell cycle distribute the BrdU to their progeny, thereby diluting it, resulting in weakly BrdU-positive cells.

Cells strongly labelled with BrdU at E10.5 were present in two discrete layers in the developing wild-type cerebral cortex at E14.5, the marginal zone at the pial surface (arrows, Fig. 3A) and the subplate (arrowheads, Fig. 3A). Between the marginal zone and the subplate, the nascent cortical plate consists of the newly arrived neurons of the future layer VI (Fig. 3A). In the *C3G*$^{gt/gt}$ mutants, by contrast, the strongly BrdU-positive cells were almost exclusively found close to the pial surface (arrows, Fig. 3B, compare with Fig. 3A), demonstrating either that preplate splitting did not occur in the *C3G*$^{gt/gt}$ mutant embryos or that the subplate cells did not survive (n=4 each for wild-type and *C3G*$^{gt/gt}$ brains). We counted strongly BrdU-positive cells in both hemispheres in the wild-type and *C3G*$^{gt/gt}$ mutant parietal cortex primordium in the marginal zone area near the pial surface versus the submarginal areas. This classification was necessary because the *C3G*$^{gt/gt}$ mutant cortex primordia did not form a recognisable marginal zone, cortical plate or subplate. The distribution of BrdU-positive cells was significantly altered in the *C3G*$^{gt/gt}$ mutants (Table 1; P<0.0001). Whereas approximately half the BrdU-positive cells populated the marginal zone and the other half the subplate in the wild type, >90% of the cells resided near the pial surface in the *C3G*$^{gt/gt}$ mutants. The remaining <10% BrdU-positive cells were scattered in various positions below the area of the marginal zone, but not arranged into a subplate. The average total number of BrdU-positive cells labelled at E10.5 and analysed at E14.5 did not differ significantly between wild-type and mutant hemispheres (39.7±4.0 versus 32.5±3.1, respectively), supporting the conclusion that mutant subplate cells did not die and that the observed difference is due to a preplate splitting defect. By contrast, later in development at E11.5 and E12.5, *C3G*$^{gt/gt}$ mutant neuroepithelial cells showed a higher rate of BrdU incorporation than wild-type cells, as we have shown previously (Voss et al.,

Table 1. Distribution of BrdU$^+$ cells in wild-type versus *C3G*$^{gt/gt}$ mutant brains labelled with BrdU at E10.5 and recovered at E14.5

Location	Wild type	*C3G*$^{gt/gt}$ mutant
Marginal zone	20.7±2.9 52.10%	29.7±3.6 91.28%
Submarginal areas	19.0±2.6 47.90%	2.8±0.7* 8.72%

Shown are the number of strongly BrdU$^+$ cells (± s.e.m.) counted at each location, also expressed as a percentage of the total. n=both hemispheres of three wild types and three *C3G*$^{gt/gt}$ mutants.
The distribution of BrdU$^+$ cells was significantly altered in the *C3G*$^{gt/gt}$ mutant (P<0.0001 by χ^2 test).
**C3G*$^{gt/gt}$ ≠ wild type in submarginal areas, P=0.0001 by one-factorial ANOVA.

2006). Similarly, marginal zone and subplate cells were distributed abnormally to the pial surface in E14.5 *C3G*$^{gt/gt}$ mutants as seen by calretinin (calbindin 2 – Mouse Genome Informatics) staining, which marks marginal zone and subplate cells in the control brains (Fig. 3, compare C with D; n=3 each for *C3G*$^{gt/gt}$ mutant and control brains). BrdU treatment at E12.5 predominantly, but not exclusively, labelled future layer VI cells, which can be seen between the marginal zone and the subplate forming the nascent cortical plate in the wild type (Fig. 3E). By contrast, *C3G*$^{gt/gt}$ mutant cells labelled at E12.5 were scattered in positions below the unsplit preplate (Fig. 3F), confirming the finding that *C3G*$^{gt/gt}$ mutant cells do not split the preplate and do not form a cortical plate.

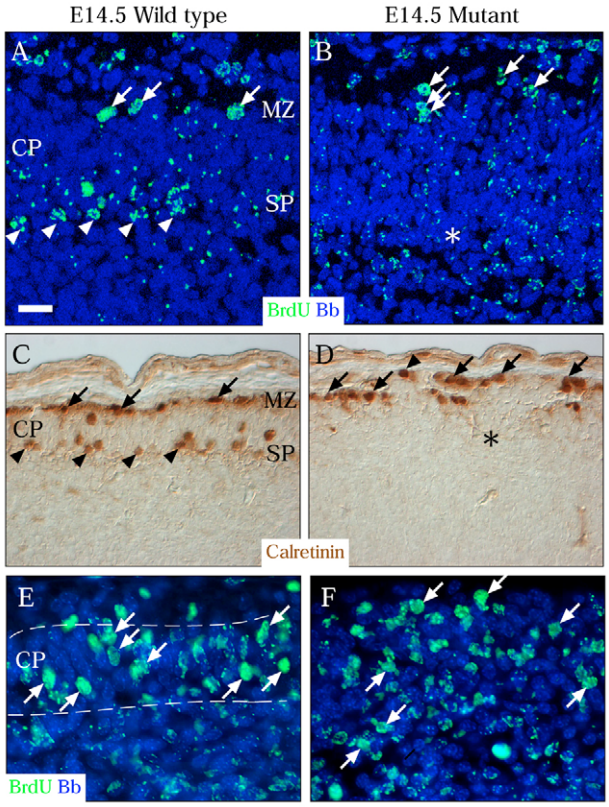

Fig. 3. The developing cerebral cortex of the *C3G*$^{gt/gt}$ mutant shows a failure of preplate splitting. (**A**,**B**) Confocal *z*-stack reconstruction of frozen sections of developing cerebral cortex of wild-type (A) and *C3G*$^{gt/gt}$ mutant (B) mouse embryos treated with BrdU at E10.5 and recovered at E14.5. Note BrdU-positive cells on the pial side (arrows in A) and below (arrowheads in A) the early cortical plate in the wild type. By contrast, in the *C3G*$^{gt/gt}$ developing cortex, BrdU-positive cells are almost exclusively found near the pial surface (arrows in B) and not in the area where the subplate would be expected (asterisk, B). (**C**,**D**) Calretinin staining (brown) of marginal zone cells (arrows) and subplate cells (arrowheads) in the wild-type (C) and *C3G*$^{gt/gt}$ mutant (D) developing cortex. Note the absence in the mutant of subplate cells in a position below the marginal zone where the subplate would be expected (asterisk in D). (**E**,**F**) Developing cerebral cortex of wild-type (E) and *C3G*$^{gt/gt}$ mutant (F) embryos treated with BrdU at E12.5 and recovered at E14.5. Note the position of the labelled wild-type cells of the future layer VI in the nascent cortical plate (arrows in E) in contrast to the disorganised position of the *C3G*$^{gt/gt}$ mutant cells (arrows in F). Note that in this experiment some preplate cells were also labelled. Labels as in Fig. 1. Scale bar: 21 μm in A; 23 μm in B; 26 μm in C,D; 17 μm in E,F.

Defective RC2-positive radial glial process anchoring and orientation in *C3G*$^{gt/gt}$ mutants in vivo

Cells of the pseudostratified neuroepithelium and radial glial cells rely for attachment to the pial surface on interaction with the basement membrane. The attachment mechanism requires laminin, β1 integrin, focal adhesion kinase and integrin-linked kinase in vivo (Beggs et al., 2003; Graus-Porta et al., 2001; Halfter et al., 2002). Furthermore, C3G has been shown to be crucial for integrin-mediated cell adhesion in fibroblasts (Voss et al., 2003). Therefore, we examined the distribution of the basement membrane protein laminin in conjunction with radial glial cell processes by staining for the marker protein RC2 (Ifaprc2) (n=3 for each genotype at each developmental stage totaling nine *C3G*$^{gt/gt}$ mutant and nine wild-type brains).

Laminin staining was continuous in the wild-type, but discontinuous in the *C3G*$^{gt/gt}$ brains, indicating disruption of the basement membrane (Fig. 2; Fig. 4, compare A,C,E,G with

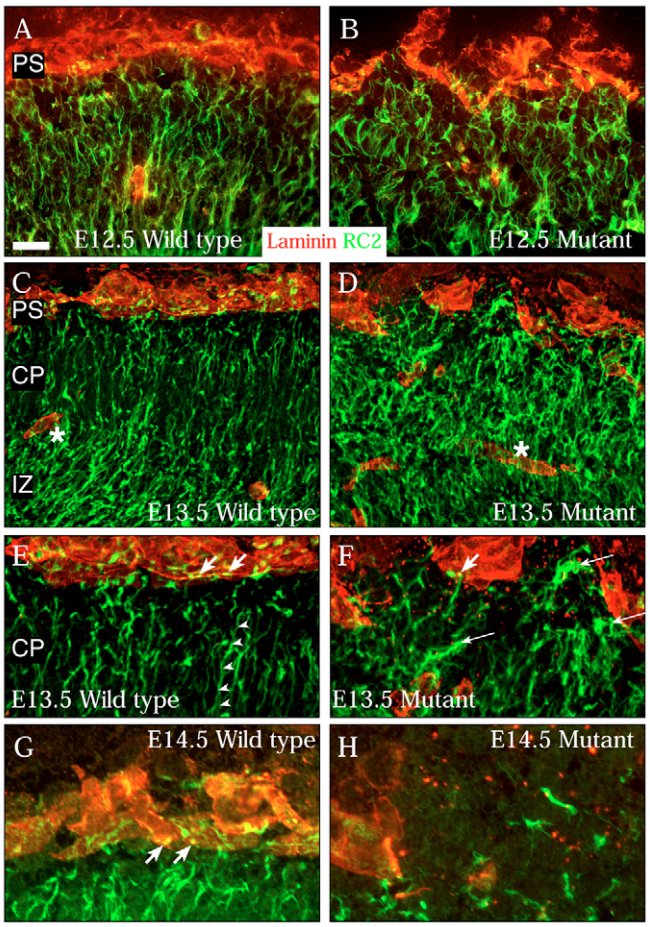

Fig. 4. Abnormal distribution of the basement membrane and of RC2-positive radial glial cells in the developing cortex of the *C3G*$^{gt/gt}$ mutant. Epifluorescence (**A**,**B**,**G**,**H**) and confocal *z*-stack reconstructions (**C-F**) of frozen sections stained for laminin (red) and RC2 (green). Wild-type (A,C,E,G) and *C3G*$^{gt/gt}$ mutant (B,D,F,H) mouse developing cerebral cortex at E12.5 to E14.5 as indicated. Wild-type radial glial processes (A,C,E,G, green, arrowheads in E) overlap (yellow, arrows in E) with basement membrane laminin (red). *C3G*$^{gt/gt}$ mutant radial glial processes are entangled (B,D,F,H, long arrows in F) and show little overlap with laminin (short arrow in F). Asterisk, blood vessel; PS, pial surface; other labels as in Fig. 1. Scale bar: 25 μm in A,B; 249 μm in C; 242 μm in D; 137 μm in E; 141 μm in F; 11 μm in G,H.

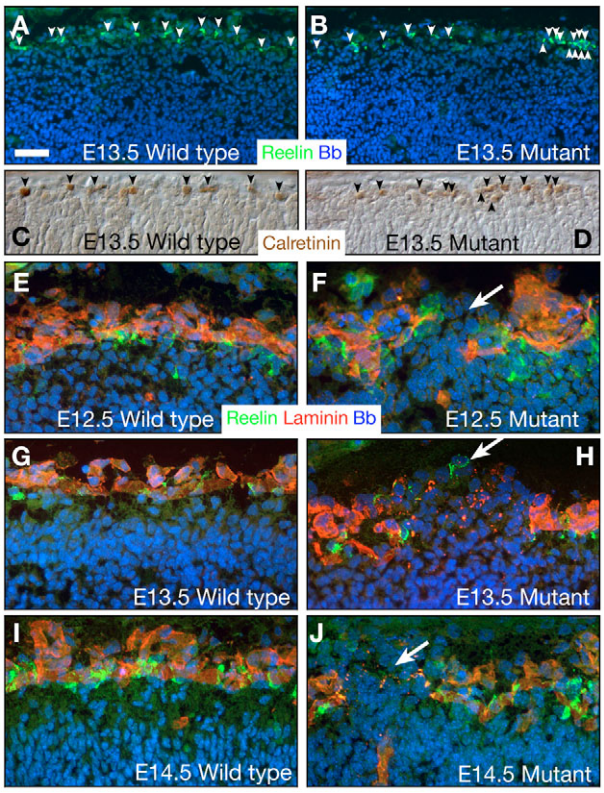

Fig. 5. Abnormal distribution of reelin-expressing marginal zone cells in the developing cortex of the *C3G$^{gt/gt}$* mutant. (**A**,**B**) Confocal images of frozen sections stained for reelin (green) and counterstained with bisbenzimide (blue). (**C**,**D**) Differential interference contrast images of paraffin sections stained for calretinin (brown). (**E-J**) Epifluorescence images of frozen sections stained for reelin (green), laminin (red) and counterstained with bisbenzimide (blue). Wild-type (A,C,E,G,I) and *C3G$^{gt/gt}$* mutant (B,D,F,H,J) mouse developing cerebral cortex at E12.5 to E14.5 as indicated. Note that cells positive for reelin (A,B) and calretinin (C,D) are evenly distributed in the wild-type (arrowheads in A,C), but not in the *C3G$^{gt/gt}$* mutant (arrowheads in B,D) developing cortex. Also note that the gaps in reelin-positive cells coincide with gaps in laminin distribution (F,H,J, arrows). Scale bar: 25 μm in A-J.

B,D,F,H). The basement membrane defect became successively more severe from E12.5 to E14.5 (Fig. 4, compare B with D and F with H). RC2 immunofluorescence, marking radial glial cell processes, was observed along cell processes with ventricular-to-pial orientation, essentially parallel to each other, in the wild type (Fig. 4A,C, arrowheads in E). By contrast, radial glial fibres in the *C3G$^{gt/gt}$* mutants were disorganised, lacked ventricular-to-pial orientation and were entangled (Fig. 4B,D and long arrows in F). Numerous small areas of overlap between RC2 and laminin staining could be observed in the wild-type tissue by confocal microscopy (arrows, Fig. 4E) and epifluorescence (arrows, Fig. 4G). These areas of laminin and RC2 overlap represent anchoring of radial glial fibres to the basement membrane. Areas of overlap between laminin and RC2 were similar in number in *C3G$^{gt/gt}$* mutants and controls at E12.5, but significantly reduced in the *C3G$^{gt/gt}$* mutants as compared with wild type at E13.5 and E14.5 (Fig. 4E-H, 25.0±4.0 versus 64.3±6.4 per 220 μm of basement membrane length, respectively; P=0.0065). Although normal numbers of RC2 and laminin double-positive areas were observed at E12.5, the basement membrane was already disorganised and tangling of radial glial processes was already manifest (Fig. 4B), suggesting that both disintegration of the basement membrane and lack of cell attachment contribute to the abnormal phenotype of *C3G$^{gt/gt}$* mutants. Lack of cell anchoring to the basement membrane, as well as the disorganisation of the radial glial processes, are possible causes of abnormal neuronal migration.

C3G$^{gt/gt}$ mutants exhibit abnormal distribution of Cajal-Retzius cells

Signalling of the ECM protein reelin to cortical neuroepithelial cells is a well-established mechanism regulating cortical neuron migration, and reelin-deficient mice exhibit a preplate splitting defect. In the developing cerebral cortex, reelin is strongly expressed by specialised cells in the marginal zone, the Cajal-Retzius neurons. Accordingly, we observed reelin immunoreactivity in evenly spaced, individual cells in the wild-type marginal zone (arrowheads, Fig. 5A). *C3G$^{gt/gt}$* mutant marginal zone cells also expressed reelin. However, they were unevenly spaced, i.e. they were congregated in some areas and absent in other areas of the pial-most aspects of the mutant cortex primordium (arrowheads, Fig. 5B; n=3 each for wild-type and *C3G$^{gt/gt}$* brains). Likewise, another marker of Cajal-Retzius cells, calretinin, showed that the *C3G$^{gt/gt}$* mutant cells were unevenly spaced (n=3 each for wild-type and *C3G$^{gt/gt}$* brains; Fig. 5, compare C with D). The unaltered expression of reelin suggests that the extracellular signalling molecule reelin is not affected by the deficiency in the intracellular signalling molecule C3G. The gaps in Cajal-Retzius cell spacing corresponded to the disruption of the basement membrane in the *C3G$^{gt/gt}$* mutant cortex at E12.5, E13.5 and E14.5 (Fig. 5E-J; n=3 for each genotype at each developmental stage totaling nine *C3G$^{gt/gt}$* mutant and nine wild-type brains). In addition to radially migrating cortical neurons, the tangentially migrating reelin-expressing Cajal-Retzius cells rely on the meningeal membranes for migration and retention in their appropriate position (Borrell and Marin, 2006; Zarbalis et al., 2007). Therefore, it is likely that the abnormal distribution of the Cajal-Retzius cells is a consequence of the disorganisation of the basement membrane.

C3G$^{gt/gt}$ mutant cortical neurons fail to migrate in organotypic brain slice culture

To enable us to observe cortical neuron migration in real time, we conducted organotypic slice cultures of *C3G$^{gt/gt}$* mutant, *C3G$^{gt/+}$* heterozygous and wild-type brains infected with eGFP-expressing virus to enable visualisation (n=3 each for *C3G$^{gt/gt}$* mutant, wild-type and *C3G$^{gt/+}$* heterozygous brains).

The E12.5 wild-type brain slices formed a robust cortical plate within the 48 hours of culture as revealed by FITC-phalloidin staining of filamentous actin (Fig. 6A). By contrast, the *C3G$^{gt/gt}$* mutant slices failed to form a cortical plate (arrows, Fig. 6B), mirroring the defects observed in vivo (Figs 1 and 2). The viral vector infects proliferating cells in the ventricular zone, which during the 48 hours of culture give rise to cells that continue to proliferate as well as to cells that differentiate into neurons. Consequently, both differentiating and proliferating cells are eGFP labelled during the imaging period. Forty-eight hours after viral infection, many eGFP-positive cells had migrated a considerable distance from the ventricular zone towards the pial surface in the wild-type slices (arrows, Fig. 6A,C). By contrast, eGFP-positive *C3G$^{gt/gt}$* mutant cells predominantly remained near the ventricular surface (arrowheads, Fig. 6B,D). Time-lapse movies of wild-type and *C3G$^{gt/gt}$* mutant brain slices (see Movies 1, 2 in the supplementary material) as well as still images (Fig. 6E-K) show a clear ventricular-to-pial orientation of the wild-type, but not of the *C3G$^{gt/gt}$* mutant, cortical neurons. The wild-type neurons were

predominantly bipolar and showed cell processes in pial or ventricular direction (arrowheads, Fig. 6E,G), whereas the *C3G*$^{gt/gt}$ mutant neurons were mostly multipolar and had three or more short processes in various directions (arrowheads, Fig. 6D,F,H-K). In the time-lapse movies it was apparent that the wild-type neurons moved along their ventricular-to-pial processes (see Movie 1 in the supplementary material), whereas the *C3G*$^{gt/gt}$ mutant neurons merely sent out small processes continually, merely to retract them again and to send out another small process in a different direction (see Movie 2 in the supplementary material). Only a very few *C3G*$^{gt/gt}$ mutant neurons moved from their position during the time-lapse imaging, although some circular movement was observed (compare Movies 1 and 2 in the supplementary material). The speed of movement of *C3G*$^{gt/gt}$ mutant cells was significantly slower than that of wild-type cells (Table 2). *C3G*$^{gt/+}$ heterozygous neurons did not exhibit a migration defect and were indistinguishable from wild type (not shown).

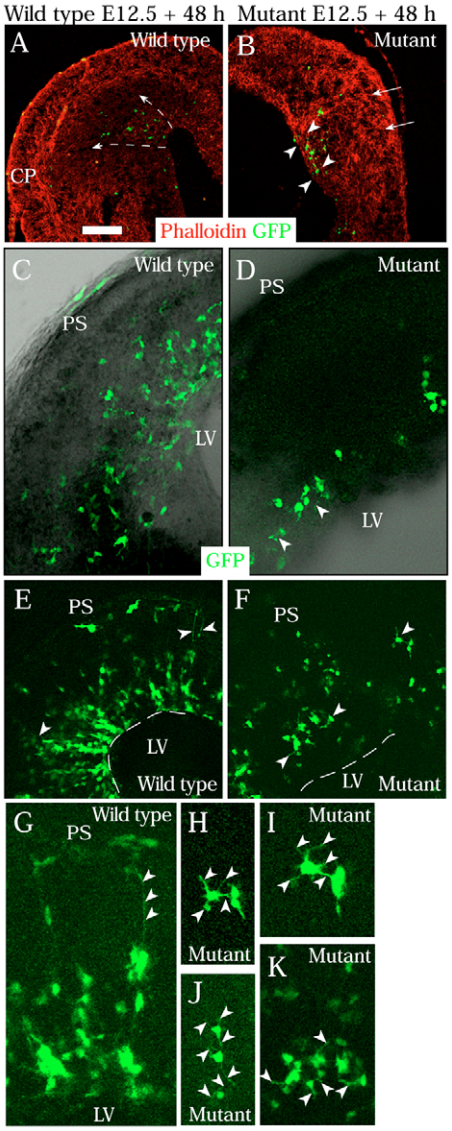

Fig. 6. *C3G*$^{gt/gt}$ mutant cortical neurons fail to migrate in ex vivo brain slice cultures. Confocal microscopy (**A**,**B**,**E-K**) and epifluorescence images (**C**,**D**) of wild-type (A,C,E,G) and *C3G*$^{gt/gt}$ mutant (B,D,F,H-K) mouse forebrain slices. Brain slices were recovered at E12.5. Proliferating neural precursor cells were infected with eGFP-expressing retrovirus to mark (green) proliferating cells and their differentiating and migrating progeny. Brain slices were cultured for 48 hours and then visualised by fluorescence microscopy. (A,B) Frozen sections of brain slices counterstained with TRITC-phalloidin marking filamentous actin reveal the structure of the cortex primordium. Note that wild-type, but not *C3G*$^{gt/gt}$ mutant, forebrain slices developed a cortical plate (A, versus arrows in B) and that wild-type (arrows in A), but not *C3G*$^{gt/gt}$ mutant (arrowheads in B), neurons migrated away from the ventricle. Wild-type neurons exhibited long radial processes (arrowheads in E,G), whereas *C3G*$^{gt/gt}$ mutant neurons had multiple short processes (arrowheads in D,F,H-K). For time-lapse, see Movies 1, 2 in the supplementary material. Dashed line, ventricular surface; CP, cortical plate; LV, lateral ventricle; PS, pial surface. Scale bar: 141 μm in A,B; 73 μm in C,D; 96 μm in E,F; 37 μm in G; 27 μm in H; 18 μm in I; 29 μm in J,K.

The eGFP-labelled cells were Emx1-positive and so of dorsal telencephalic origin in the wild-type and *C3G*$^{gt/gt}$ mutant brains and were negative for GABA, thereby excluding interneuron identity (data not shown). Therefore, the absence of radial orientation of *C3G*$^{gt/gt}$ mutant neurons cannot be attributed to an interneuron identity and is instead an abnormal function of dorsal telencephalic neurons, which ordinarily migrate predominantly radially (Tan and Breen, 1993; Tan et al., 1998).

C3G$^{gt/gt}$ mutant cortical neurons fail to migrate on complex or defined matrix in vitro

Dorsal telencephalic neuroepithelium explant cultures were established to monitor cortical neuron migration on a complex ECM or recombinant laminin. In wild-type cultures, cell processes emanated radially and neurons emerged and migrated away from the explants along the cell processes after 3 days (arrowheads, Fig. 7A). After 6 days of culture, wild-type explants were surrounded by a corona of radially migrating neurons (arrowheads, Fig. 7C). In addition to migration along explant-derived cell processes, wild-type cells also migrated on complex matrix independently of cell processes. By contrast, *C3G*$^{gt/gt}$ telencephalic explants did not give rise to processes or migrating cells throughout the culture period (Fig. 7, compare A with B and C with D) (n=14 each for wild-type, *C3G*$^{gt/+}$ and *C3G*$^{gt/gt}$ brains). Similarly, on the defined laminin substrate, *C3G*$^{gt/gt}$ explants failed to generate processes or migrating neurons, whereas wild-type explants exhibited both processes and migrating neurons (Fig. 7, compare E with F). *C3G*$^{gt/+}$ heterozygous explants were indistinguishable from wild-type explants (not shown). As *C3G*$^{gt/gt}$ mutant cells were unable to send out processes, we can only comment on their ability for cell-process-independent migration in this assay and conclude that, unlike wild-type cells, *C3G*$^{gt/gt}$ mutant cells were incapable of migration on complex or defined matrix. In time-lapse movies, wild-type cortical neurons were observed migrating centrifugally away from the explants. Some wild-type cells first moved away, then towards the explants and finally reverted to centrifugal migration. A migration velocity of 10 μm/hour was observed (Fig. 7I-K and see Movie 3 in the supplementary material). The speed of 10 μm/hour is similar to that

Table 2. Neuronal migration speed in brain slice cultures

Migration	Wild type	*C3G*$^{gt/gt}$ mutant	*P* value
Fast-moving cells	10.6±0.5	4.9±0.9	*P*<0.0001
Slow-moving cells	4.6±0.5	2.7±0.5	*P*=0.0008
All cells	7.6±0.8	3.8±0.3	*P*<0.0001

Mean speed (μm/hour) ± s.e.m. in three wild types and three *C3G*$^{gt/gt}$ mutants were assessed. The migration speed of the 10-12 most-mobile cells was recorded per animal. Data were analysed by one-factorial ANOVA.

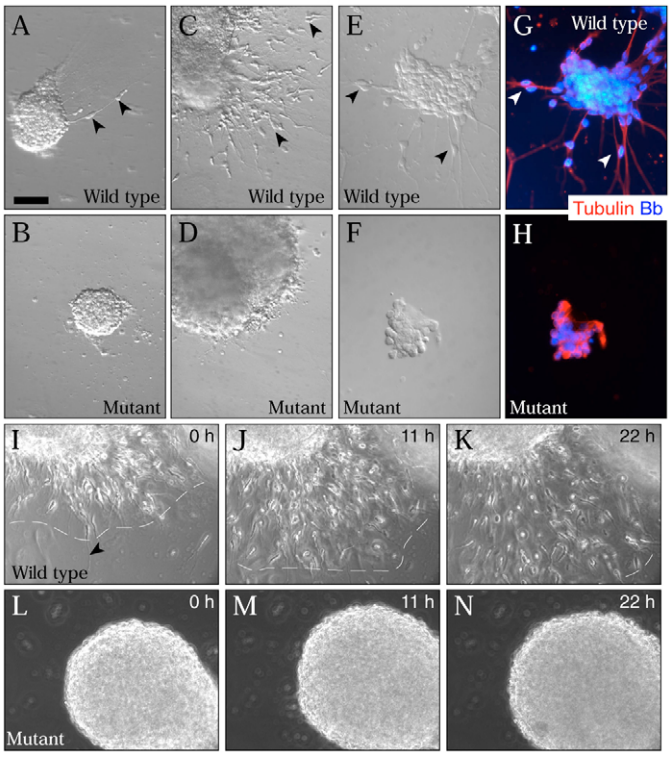

Fig. 7. *C3G*$^{gt/gt}$ mutant cortical neuroepithelial cells fail to extend processes and fail to migrate on complex or defined matrix in vitro. (**A-N**) Cortical neuroepithelial explants of wild-type (A,C,E,G,I-K) or *C3G*$^{gt/gt}$ mutant (B,D,F,H,L-N) E10.5 mouse embryos were plated on complex extracellular matrix (A-D,I-N) or recombinant laminin (E-H) and cultured; (A,B) day 3 of culture, (C-H) day 6, (I-N) day 3 to day 4. For time-lapse, see Movies 3, 4 in the supplementary material. (G,H) Cultures on laminin were stained for the neuronal marker type III β-tubulin (red) and counterstained with bisbenzimide (blue). Differential interference contrast images (A-F), epifluorescence images (G,H) and time-lapse phase-contrast images (I-N). (A,C,E,G,I) Processes and migrating neurons were seen in wild-type (arrowheads) but not in *C3G*$^{gt/gt}$ mutant cultures. Dashed line, migration front. Scale bar: 72 μm in A-D; 37 μm in E-H; 70 μm in I-N.

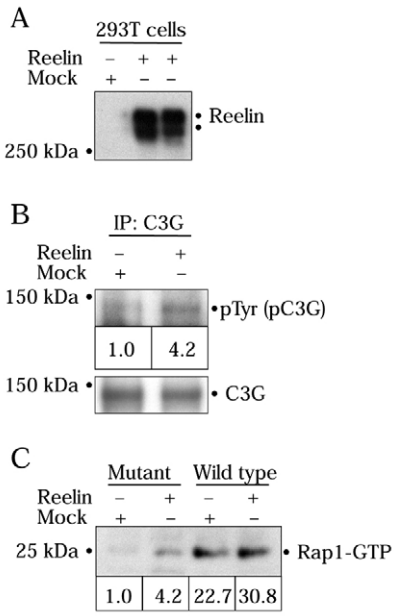

Fig. 8. C3G activation in response to reelin. (**A**) Reelin is present in the supernatant of 293T cells transfected with a reelin expression construct, but not in the supernatant of cells transfected with an empty vector (mock). (**B**) Immunoblot probed for tyrosine phosphorylated protein (pC3G) and reprobed for total C3G (lower panel) in lysates of E16.5 wild-type cortical neurons treated with supernatant of reelin-expressing or mock transfected 293T cells for 15 minutes and precipitated with anti-C3G antibody. Numbers below lanes indicate relative densitometry readings corrected for total C3G. (**C**) Immunoblot probed for Rap1 in lysate of neural precursor cells treated with reelin or control supernatant (mock) for 24 hours, then subjected to RalGDS-Rap1-binding domain affinity purification of GTP-loaded Rap1. Numbers below lanes indicate relative densitometry readings.

observed previously for cortical neurons (Noctor et al., 2004). By contrast, *C3G*$^{gt/gt}$ mutant cortical neuroepithelial explants showed a complete absence of migration. Note, however, that although no cells migrated out of the *C3G*$^{gt/gt}$ explants, movement within the *C3G*$^{gt/gt}$ explants was apparent and the explants increased in size during the culture period (Fig. 7L-N and see Movie 4 in the supplementary material; n=8 each for wild-type, *C3G*$^{gt/+}$ and *C3G*$^{gt/gt}$ brains).

Like wild-type, *C3G*$^{gt/gt}$ mutant explant cells expressed the neuronal marker β-tubulin type III (Fig. 7G,H). Moreover, isolated wild-type and *C3G*$^{gt/gt}$ mutant cortical neural precursor cells formed similar percentages of neurons when induced to differentiate on laminin in vitro (not shown). Therefore, *C3G*$^{gt/gt}$ neuroepithelial cells differentiated into cells expressing neuronal marker proteins, but failed to send out processes and were unable to migrate on laminin or complex matrix. The *C3G* mutant cell attachment and migration defects observed in explant cultures are more severe than the migration defects observed in vivo or in brain slice cultures, presumably because the substrate offered for attachment in the explant cultures is less supportive than the extracellular environment in the brain. It is noteworthy, however, that the same substrate is sufficient for the attachment and migration of wild-type cells.

C3G mediates reelin-induced Rap1 activation

Since the preplate splitting defect in the *C3G*$^{gt/gt}$ mutant embryos resembles the preplate splitting defect in reelin mutant mice, we postulated that C3G might be an effector of reelin signalling. Indeed, C3G is phosphorylated (activated) in response to reelin stimulation in E16.5 wild-type, but not in *Dab1* mutant, cortical neurons; furthermore, the downstream target of C3G activation, Rap1 is loaded with GTP upon reelin stimulation (Ballif et al., 2004). As previously shown by others (Ballif et al., 2004), we observed that E16.5 wild-type cortical neurons treated with reelin (Fig. 8A) exhibited induction of C3G tyrosine phosphorylation (Fig. 8B) corresponding to C3G activation. As the major effect of C3G activation is Rap1 GTP loading [activation (Ohba et al., 2001)], we examined Rap1 activation in *C3G* mutant and wild-type cells. To obtain sufficient amounts of material for this experiment we used E10.5 neural precursor cells expanded in vitro as described previously (Voss et al., 2006). After 4 hours of mitogen withdrawal, E10.5 neural precursor cells were treated with or without reelin. GTP loading of Rap1 (activation) was higher in mock-treated wild-type cells than in mock-treated *C3G* mutant cells (Fig. 8C). Moreover, reelin-treated wild-type cells showed higher levels of Rap1 GTP loading than *C3G* mutant cells. Reelin-treated *C3G*

mutant cells had 5-fold lower levels of GTP-loaded Rap1, even compared with unstimulated wild-type cells (Fig. 8C). *C3G* mutant cells responded to reelin stimulation with modest levels of Rap1 GTP loading, which may be attributed to the fact that our $C3G^{gt}$ allele is not a null allele and produces approximately 5% normal C3G protein (Voss et al., 2003).

In summary, C3G is activated by reelin and is required for Rap1 activation in response to reelin. *C3G* mutant mice phenocopy the reelin mutant preplate splitting defect. Together, our findings suggest that C3G is an essential effector of reelin signalling in cortical development.

DISCUSSION

In the present study, we have shown that $C3G^{gt/gt}$ hypomorphic mutant mice have severe defects in cortical development. The cortical malformations resulting from insufficient C3G fall into two distinct classes (Fig. 9).

Firstly, C3G deficiency causes a fundamental defect in one of the earliest steps of cortical neuron migration, i.e. C3G-deficient cortical neurons fail to split the cortical preplate. The first C3G-deficient post-mitotic neurons are positioned near the pial surface and form an apparently normal preplate. However, prospective layer VI neurons fail to migrate into the preplate and therefore fail to split the preplate into marginal zone and subplate. Instead, the second cohort remains below the preplate. This phenotype has previously been found in four cases only, all mutations of members of the reelin signalling pathway.

Secondly, we found areas of the developing cortex where the basement membrane was disrupted and groups of cortical neurons had invaded the marginal zone. This phenotype is similar to the undulating cortex previously observed in mice with mutations causing a disruption of the basement membrane or disruption of the interactions of cells with the basement membrane.

The cortical preplate splitting defect in $C3G^{gt/gt}$ mutants

The defect in cortical preplate splitting in $C3G^{gt/gt}$ mutant embryos is similar to defects found in mice carrying mutations in the reelin gene (D'Arcangelo et al., 1995; Sheppard and Pearlman, 1997), *ApoER2* (*Lrp8* – Mouse Genome Informatics) and *Vldlr* (Trommsdorff et al., 1999), *Src* and *Fyn* (Kuo et al., 2005) and *Dab1* (Howell et al., 1997; Rice et al., 1998; Sheldon et al., 1997). Mutations in these genes of the reelin signalling pathway cause preplate splitting defects and subsequently show defects in cortical layer formation.

Signalling through the reelin/ApoER2/Vldlr/Src/Fyn/Dab1 signalling pathway (D'Arcangelo et al., 1995; Howell et al., 1997; Kuo et al., 2005; Sheldon et al., 1997; Trommsdorff et al., 1999) is required for the development of normal cortical lamination. However, only the proximal aspects of this signalling pathway and some, but not all, downstream events are well understood (D'Arcangelo, 2006; Tissir and Goffinet, 2003). Reelin binding to ApoER2/Vldlr activates the Src family kinases Src and Fyn, which leads to Dab1 phosphorylation. How these events are connected to the downstream effectors, such as actin skeleton reorganisation and microtubule motor complex function, is unknown (D'Arcangelo, 2006; Tissir and Goffinet, 2003). Although additional components of the reelin signalling pathway have been identified in vitro in recent years, their function in neuronal migration in vivo has not been elucidated (D'Arcangelo, 2006). In particular, it was recently reported that C3G phosphorylation is the first phosphorylation event in reelin-stimulated neurons, along with Dab1 phosphorylation (Ballif et al., 2004). However, that study did not address whether or not C3G is functionally relevant to neuronal migration. We provide direct evidence here that lack of C3G causes similar defects in early corticogenesis to reelin mutation. Furthermore, we show that in the C3G-deficient state, the effects of reelin mediated by C3G, namely increased Rap1 GTP loading, are largely abrogated. As C3G is required for filopodia formation in fibroblasts (Radha et al., 2007) and Rap1 for protrusion formation in a number of cell lines (Arthur et al., 2004), reelin-induced C3G-mediated Rap1 activation may be required for cell process extension.

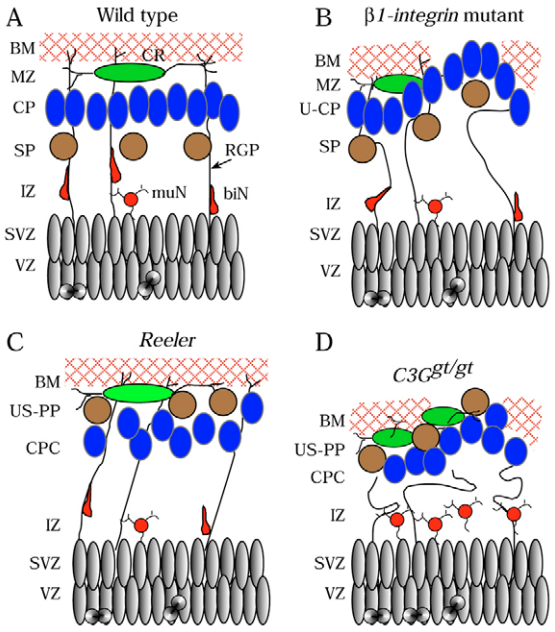

Fig. 9. Comparison of the $C3G^{gt/gt}$ mutant phenotype with the Reeler phenotype and the nervous-system-specific β1 integrin conditional mutant phenotype. (**A**) At E14.5, the developing wild-type mouse cortex consists of ventricular (VZ), subventricular (SVZ) and intermediate (IZ) zones, subplate (SP), the nascent cortical plate (CP), marginal zone (MZ) and has a continuous basement membrane (BM) at its pial surface. Cajal-Retzius (CR, green) cells expressing reelin are located in the marginal zone. Radial glial processes (RGP) extend from the ventricular zone to the basement membrane at the pial surface, where they are anchored with endfeet to the extracellular matrix protein lattice. Migrating bipolar neurons (biN) are guided by radial glial processes and may transiently become multipolar (muN). (**B**) β1 integrin deficiency in the brain leads to a disruption of the basement membrane, loss of parallel radial glial process orientation and loss of endfeet anchoring, as well as an undulating cortical plate (U-CP) with invasion of the marginal zone by cortical plate cells (Graus-Porta et al., 2001). (**C**) Loss of reelin leads to a lack of reelin expression in the Cajal-Retzius cells and to a failure of cortical plate cells to split the preplate (PP) into marginal zone and subplate, resulting in an unsplit preplate (US-PP) and the stacking of cortical plate cells (CPC) below the unsplit preplate (Sheppard and Pearlman, 1997). In addition, lack of reelin leads to oblique orientation of the radial glial processes. (**D**) The $C3G^{gt/gt}$ mutant phenotype combines all elements of the Reeler phenotype and the β1 integrin mutant phenotype: lack of preplate splitting, the stacking of cortical plate cells below the unsplit preplate, disruption of the basement membrane, invasion of the marginal zone and pericerebral space by cortical plate cells, loss of radial glial process orientation and loss of endfeet anchoring. In addition, lack of C3G leads to an accumulation of migrating neurons in the multipolar stage.

Recent detailed studies have shown that there are multiple modes of neuron migration and that migration might involve a number of discrete stages. Initially, neurons leave the ventricular zone by a process of somal translocation, in which neurons retain connection to the pial surface but lose connection to cells lining the ventricle and retract to the pia. Subsequently, neurons move away from the ventricles by locomotion, a process by which cells migrate along radial glia, but may also leave glia and reside temporally in the subventricular zone before resuming migration. While dissociated from the radial glia, these cells have a characteristic multipolar phenotype (Noctor et al., 2004; Tabata and Nakajima, 2003). Interestingly, the majority of C3G-deficient neurons display a multipolar morphology and are arrested in migration in brain slice cultures. This phenotype is reminiscent of the dominant-negative and RNAi depletion phenotypes of filamin A and Lis1 (Pafah1β1 – Mouse Genome Informatics), which both cause arrest at the multipolar stage of cortical neuron migration (Nagano et al., 2004; Tsai et al., 2005). Failure to return to the bipolar morphology may impede further migration. It is therefore possible that C3G might provide a link between the well-known upstream aspects of the reelin signalling pathway and effector events involving filamin A and Lis1 function in the contexts of the actin cytoskeleton and the microtubule motor complex.

The disorientation of the radial glial processes in the *C3G*$^{gt/gt}$ mutants surpasses that observed in Reeler mutants. In Reeler mutants, radial glial processes span the ventricular-to-pial extent of the developing cortex at an oblique angle (Hartfuss et al., 2003; Luque et al., 2003; Magdaleno and Curran, 2001). In *C3G*$^{gt/gt}$ mutants, radial glial processes are completely disorganised suggesting, in addition to a defect in reelin signalling, the failure of a second cellular process, as discussed below.

Defective interaction between neuroepithelial cells and the basement membrane in *C3G*$^{gt/gt}$ mutants

In addition to the overlap between the *C3G*$^{gt/gt}$ and the reelin mutant phenotypes, the *C3G*$^{gt/gt}$ mutant phenotype shows similarities to the abnormalities caused by disruption of the basement membrane (Halfter et al., 2002) or failure to attach to the basement membrane (Beggs et al., 2003; Graus-Porta et al., 2001; Niewmierzycka et al., 2005). For example, mouse foetuses with nervous-system-specific deletion of the β1 integrin gene (*Itgb1*) show a discontinuous basement membrane as evidenced by discontinuous laminin staining. Moreover, they exhibit invasion of the marginal zone by cortical plate neurons (Graus-Porta et al., 2001). Like the β1 integrin-deficient developing cerebral cortex, the *C3G*$^{gt/gt}$ mutant cortex primordium exhibits discontinuity of laminin deposits in the basement membrane and invasion of the marginal zone and even of the pericerebral space by cortical neurons, suggesting a total collapse of basement membrane function. As interactions of laminins with integrin receptors are required to localise laminin at appropriate sites for basement membrane assembly (Schwarzbauer, 1999), and as C3G is required for integrin signalling and function (Arai et al., 2001; Arai et al., 1999; Uemura and Griffin, 1999; Voss et al., 2003; Voss et al., 2006), the observed discontinuity of the basement membrane is likely to be the result of a lack of integrin signalling in the absence of C3G.

Notably, RC2-positive radial glia cell fibres, which are important for cortical neuron migration, largely fail to connect to the discontinuous laminin deposits present in the *C3G*$^{gt/gt}$ mutants. Perhaps as a consequence of their failure to connect to the ECM, the *C3G*$^{gt/gt}$ mutant radial glia fibres are disorganised, entangled and lack ventricular-to-pial orientation. Furthermore, our in vitro findings show that C3G is required for neuron-ECM interaction for process extension and migration on ECM. Previous reports have established that C3G is activated in response to the engagement of number of different substrates and different integrin heterodimers in a variety of cell types (Arai et al., 2001; Arai et al., 1999; Uemura and Griffin, 1999). Functionally, C3G is essential for embryonic fibroblast cell adhesion and regulation of migration (Ohba et al., 2001; Voss et al., 2003) and for the establishment/maintenance of β1 integrin- and paxillin-positive focal adhesions in embryonic fibroblasts (Voss et al., 2003). Furthermore, laminin-induced Rap1 activation is C3G dependent in differentiating neural precursor cells (Voss et al., 2006). Our current data show that, similar to fibroblasts, neurons have an essential requirement for C3G for interaction with ECM proteins.

In conclusion, we have shown that the Ras signalling molecule C3G is crucial for cortical neuron migration. Our results are consistent with the hypothesis that reelin signalling and integrin signalling converge on C3G activity in migrating cortical neurons. The *C3G* mutant phenotype combines both elements – reelin loss and integrin loss – and therefore exceeds either of these mutants in severity.

We thank S. Michajlovic, N. Ashman and A. Morcom for technical assistance, T. Kilpatrick for discussion, and F. Gage and T. Curran for reagents. This work was supported by the Walter and Eliza Hall Institute of Medical Research and by the Australian NHMRC.

Supplementary material

Supplementary material for this article is available at http://dev.biologists.org/cgi/content/full/135/12/2139/DC1

References

Arai, A., Nosaka, Y., Kohsaka, H., Miyasaka, N. and Miura, O. (1999). CrkL activates integrin-mediated hematopoietic cell adhesion through the guanine nucleotide exchange factor C3G. *Blood* **93**, 3713-3722.

Arai, A., Nosaka, Y., Kanda, E., Yamamoto, K., Miyasaka, N. and Miura, O. (2001). Rap1 is activated by erythropoietin or interleukin-3 and is involved in regulation of beta1 integrin-mediated hematopoietic cell adhesion. *J. Biol. Chem.* **276**, 10453-10462.

Arthur, W. T., Quilliam, L. A. and Cooper, J. A. (2004). Rap1 promotes cell spreading by localizing Rac guanine nucleotide exchange factors. *J. Cell Biol.* **167**, 111-122.

Ayala, R., Shu, T. and Tsai, L. H. (2007). Trekking across the brain: the journey of neuronal migration. *Cell* **128**, 29-43.

Ballif, B. A., Arnaud, L., Arthur, W. T., Guris, D., Imamoto, A. and Cooper, J. A. (2004). Activation of a Dab1/CrkL/C3G/Rap1 pathway in Reelin-stimulated neurons. *Curr. Biol.* **14**, 606-610.

Bayer, S. A. and Altman, J. (1991). *Neocortical Development*. New York: Raven.

Beggs, H. E., Schahin-Reed, D., Zang, K., Goebbels, S., Nave, K. A., Gorski, J., Jones, K. R., Sretavan, D. and Reichardt, L. F. (2003). FAK deficiency in cells contributing to the basal lamina results in cortical abnormalities resembling congenital muscular dystrophies. *Neuron* **40**, 501-514.

Bielle, F., Griveau, A., Narboux-Neme, N., Vigneau, S., Sigrist, M., Arber, S., Wassef, M. and Pierani, A. (2005). Multiple origins of Cajal-Retzius cells at the borders of the developing pallium. *Nat. Neurosci.* **8**, 1002-1012.

Borrell, V. and Marin, O. (2006). Meninges control tangential migration of hem-derived Cajal-Retzius cells via CXCL12/CXCR4 signaling. *Nat. Neurosci.* **9**, 1284-1293.

Chan, C. H., Godinho, L. N., Thomaidou, D., Tan, S. S., Gulisano, M. and Parnavelas, J. G. (2001). Emx1 is a marker for pyramidal neurons of the cerebral cortex. *Cereb. Cortex* **11**, 1191-1198.

D'Arcangelo, G. (2006). Reelin mouse mutants as models of cortical development disorders. *Epilepsy Behav.* **8**, 81-90.

D'Arcangelo, G., Miao, G. G., Chen, S. C., Soares, H. D., Morgan, J. I. and Curran, T. (1995). A protein related to extracellular matrix proteins deleted in the mouse mutant reeler. *Nature* **374**, 719-723.

D'Arcangelo, G., Nakajima, K., Miyata, T., Ogawa, M., Mikoshiba, K. and Curran, T. (1997). Reelin is a secreted glycoprotein recognized by the CR-50 monoclonal antibody. *J. Neurosci.* **17**, 23-31.

Graus-Porta, D., Blaess, S., Senften, M., Littlewood-Evans, A., Damsky, C., Huang, Z., Orban, P., Klein, R., Schittny, J. C. and Muller, U. (2001). Beta1-class integrins regulate the development of laminae and folia in the cerebral and cerebellar cortex. *Neuron* **31**, 367-379.

Gupta, A., Tsai, L. H. and Wynshaw-Boris, A. (2002). Life is a journey: a genetic look at neocortical development. *Nat. Rev. Genet.* **3**, 342-355.

Halfter, W., Dong, S., Yip, Y. P., Willem, M. and Mayer, U. (2002). A critical function of the pial basement membrane in cortical histogenesis. *J. Neurosci.* **22**, 6029-6040.
Hartfuss, E., Forster, E., Bock, H. H., Hack, M. A., Leprince, P., Luque, J. M., Herz, J., Frotscher, M. and Gotz, M. (2003). Reelin signaling directly affects radial glia morphology and biochemical maturation. *Development* **130**, 4597-4609.
Herrick, T. M. and Cooper, J. A. (2002). A hypomorphic allele of dab1 reveals regional differences in reelin-Dab1 signaling during brain development. *Development* **129**, 787-796.
Howell, B. W., Hawkes, R., Soriano, P. and Cooper, J. A. (1997). Neuronal position in the developing brain is regulated by mouse disabled-1. *Nature* **389**, 733-737.
Ichiba, T., Kuraishi, Y., Sakai, O., Nagata, S., Groffen, J., Kurata, T., Hattori, S. and Matsuda, M. (1997). Enhancement of guanine-nucleotide exchange activity of C3G for Rap1 by the expression of Crk, CrkL, and Grb2. *J. Biol. Chem.* **272**, 22215-22220.
Knudsen, B. S., Feller, S. M. and Hanafusa, H. (1994). Four proline-rich sequences of the guanine-nucleotide exchange factor C3G bind with unique specificity to the first Src homology 3 domain of Crk. *J. Biol. Chem.* **269**, 32781-32787.
Kuo, G., Arnaud, L., Kronstad-O'Brien, P. and Cooper, J. A. (2005). Absence of Fyn and Src causes a reeler-like phenotype. *J. Neurosci.* **25**, 8578-8586.
Liesi, P. (1985). Do neurons in the vertebrate CNS migrate on laminin? *EMBO J.* **4**, 1163-1170.
Luque, J. M., Morante-Oria, J. and Fairen, A. (2003). Localization of ApoER2, VLDLR and Dab1 in radial glia: groundwork for a new model of reelin action during cortical development. *Brain Res. Dev. Brain Res.* **140**, 195-203.
Magdaleno, S. M. and Curran, T. (2001). Brain development: integrins and the Reelin pathway. *Curr. Biol.* **11**, R1032-R1035.
Merson, T. D., Dixon, M. P., Collin, C., Rietze, R. L., Bartlett, P. F., Thomas, T. and Voss, A. K. (2006). The transcriptional coactivator Querkopf controls adult neurogenesis. *J. Neurosci.* **26**, 11359-11370.
Nadarajah, B., Brunstrom, J. E., Grutzendler, J., Wong, R. O. and Pearlman, A. L. (2001). Two modes of radial migration in early development of the cerebral cortex. *Nat. Neurosci.* **4**, 143-150.
Nagano, T., Morikubo, S. and Sato, M. (2004). Filamin A and FILIP (Filamin A-Interacting Protein) regulate cell polarity and motility in neocortical subventricular and intermediate zones during radial migration. *J. Neurosci.* **24**, 9648-9657.
Niewmierzycka, A., Mills, J., St-Arnaud, R., Dedhar, S. and Reichardt, L. F. (2005). Integrin-linked kinase deletion from mouse cortex results in cortical lamination defects resembling cobblestone lissencephaly. *J. Neurosci.* **25**, 7022-7031.
Noctor, S. C., Flint, A. C., Weissman, T. A., Dammerman, R. S. and Kriegstein, A. R. (2001). Neurons derived from radial glial cells establish radial units in neocortex. *Nature* **409**, 714-720.
Noctor, S. C., Martinez-Cerdeno, V., Ivic, L. and Kriegstein, A. R. (2004). Cortical neurons arise in symmetric and asymmetric division zones and migrate through specific phases. *Nat. Neurosci.* **7**, 136-144.
Ohba, Y., Ikuta, K., Ogura, A., Matsuda, J., Mochizuki, N., Nagashima, K., Kurokawa, K., Mayer, B. J., Maki, K., Miyazaki, J. et al. (2001). Requirement for C3G-dependent Rap1 activation for cell adhesion and embryogenesis. *EMBO J.* **20**, 3333-3341.
Olson, E. C. and Walsh, C. A. (2002). Smooth, rough and upside-down neocortical development. *Curr. Opin. Genet. Dev.* **12**, 320-327.
Palmer, T. D., Markakis, E. A., Willhoite, A. R., Safar, F. and Gage, F. H. (1999). Fibroblast growth factor-2 activates a latent neurogenic program in neural stem cells from diverse regions of the adult CNS. *J. Neurosci.* **19**, 8487-8497.
Radha, V., Rajanna, A., Mitra, A., Rangaraj, N. and Swarup, G. (2007). C3G is required for c-Abl-induced filopodia and its overexpression promotes filopodia formation. *Exp. Cell Res.* **313**, 2476-2492.
Rice, D. S., Sheldon, M., D'Arcangelo, G., Nakajima, K., Goldowitz, D. and Curran, T. (1998). Disabled-1 acts downstream of Reelin in a signaling pathway that controls laminar organization in the mammalian brain. *Development* **125**, 3719-3729.
Schwarzbauer, J. (1999). Basement membranes: putting up the barriers. *Curr. Biol.* **9**, R242-R244.
Sheldon, M., Rice, D. S., D'Arcangelo, G., Yoneshima, H., Nakajima, K., Mikoshiba, K., Howell, B. W., Cooper, J. A., Goldowitz, D. and Curran, T. (1997). Scrambler and yotari disrupt the disabled gene and produce a reeler-like phenotype in mice. *Nature* **389**, 730-733.
Sheppard, A. M. and Pearlman, A. L. (1997). Abnormal reorganization of preplate neurons and their associated extracellular matrix: an early manifestation of altered neocortical development in the reeler mutant mouse. *J. Comp. Neurol.* **378**, 173-179.
Sheppard, A. M., Hamilton, S. K. and Pearlman, A. L. (1991). Changes in the distribution of extracellular matrix components accompany early morphogenetic events of mammalian cortical development. *J. Neurosci.* **11**, 3928-3942.
Stewart, G. R. and Pearlman, A. L. (1987). Fibronectin-like immunoreactivity in the developing cerebral cortex. *J. Neurosci.* **7**, 3325-3333.
Tabata, H. and Nakajima, K. (2003). Multipolar migration: the third mode of radial neuronal migration in the developing cerebral cortex. *J. Neurosci.* **23**, 9996-10001.
Takiguchi-Hayashi, K., Sekiguchi, M., Ashigaki, S., Takamatsu, M., Hasegawa, H., Suzuki-Migishima, R., Yokoyama, M., Nakanishi, S. and Tanabe, Y. (2004). Generation of reelin-positive marginal zone cells from the caudomedial wall of telencephalic vesicles. *J. Neurosci.* **24**, 2286-2295.
Tan, S. S. and Breen, S. (1993). Radial mosaicism and tangential cell dispersion both contribute to mouse neocortical development. *Nature* **362**, 638-640.
Tan, S. S., Kalloniatis, M., Sturm, K., Tam, P. P., Reese, B. E. and Faulkner-Jones, B. (1998). Separate progenitors for radial and tangential cell dispersion during development of the cerebral neocortex. *Neuron* **21**, 295-304.
Tanaka, S., Morishita, T., Hashimoto, Y., Hattori, S., Nakamura, S., Shibuya, M., Matuoka, K., Takenawa, T., Kurata, T. and Nagashima, K. (1994). C3G, a guanine nucleotide-releasing protein expressed ubiquitously, binds to the Src homology 3 domains of CRK and GRB2/ASH proteins. *Proc. Natl. Acad. Sci. USA* **91**, 3443-3447.
Thomas, T. and Dziadek, M. (1993a). Capacity to form choroid plexus-like cells in vitro is restricted to specific regions of the mouse neural ectoderm. *Development* **117**, 253-262.
Thomas, T. and Dziadek, M. (1993b). Genes coding for basement membrane glycoproteins laminin, nidogen, and collagen IV are differentially expressed in the nervous system and by epithelial, endothelial, and mesenchymal cells of the mouse embryo. *Exp. Cell Res.* **208**, 54-67.
Thomas, T., Voss, A. K., Chowdhury, K. and Gruss, P. (2000). Querkopf, a MYST family histone acetyltransferase, is required for normal cerebral cortex development. *Development* **127**, 2537-2548.
Tissir, F. and Goffinet, A. M. (2003). Reelin and brain development. *Nat. Rev. Neurosci.* **4**, 496-505.
Trommsdorff, M., Gotthardt, M., Hiesberger, T., Shelton, J., Stockinger, W., Nimpf, J., Hammer, R. E., Richardson, J. A. and Herz, J. (1999). Reeler/Disabled-like disruption of neuronal migration in knockout mice lacking the VLDL receptor and ApoE receptor 2. *Cell* **97**, 689-701.
Tsai, J. W., Chen, Y., Kriegstein, A. R. and Vallee, R. B. (2005). LIS1 RNA interference blocks neural stem cell division, morphogenesis, and motility at multiple stages. *J. Cell Biol.* **170**, 935-945.
Uemura, N. and Griffin, J. D. (1999). The adapter protein Crkl links Cbl to C3G after integrin ligation and enhances cell migration. *J. Biol. Chem.* **274**, 37525-37532.
Voss, A. K., Thomas, T., Petrou, P., Anastassiadis, K., Scholer, H. and Gruss, P. (2000). Taube nuss is a novel gene essential for the survival of pluripotent cells of early mouse embryos. *Development* **127**, 5449-5461.
Voss, A. K., Gruss, P. and Thomas, T. (2003). The guanine nucleotide exchange factor C3G is necessary for the formation of focal adhesions and vascular maturation. *Development* **130**, 355-367.
Voss, A. K., Krebs, D. L. and Thomas, T. (2006). C3G regulates the size of the cerebral cortex neural precursor population. *EMBO J.* **25**, 3652-3663.
Zarbalis, K., Siegenthaler, J. A., Choe, Y., May, S. R., Peterson, A. S. and Pleasure, S. J. (2007). Cortical dysplasia and skull defects in mice with a Foxc1 allele reveal the role of meningeal differentiation in regulating cortical development. *Proc. Natl. Acad. Sci. USA* **104**, 14002-14007.